Analytical Methods

ROYAL SOCIETY OF CHEMISTRY

CRITICAL REVIEW

View Article Online
View Journal



Cite this: DOI: 10.1039/d6ay00304d

# Affinity sensors for L-lactate and lactate dehydrogenase

Longyu Li and Juewen Liu *

L-lactate is a key metabolite and biomarker with wide range of concentrations across human body fluids. Accurate and continuous monitoring of human lactate and lactate dehydrogenase (LDH) concentration is essential for sports, clinical, and diagnostic applications. Conventional enzyme-based sensors employing lactate oxidase or lactate dehydrogenase dominate current practice but face inherent limitations in stability, operating conditions, and production cost. On the other hand, affinity-based sensors can be promising alternatives. This review highlights recent advancements in affinity sensors for L-lactate and LDH detection such as the first reported L-lactate aptamers, their selection and characterization, and their integration into wearable electrochemical devices. Affinity sensors for lactate dehydrogenase (LDH) detection, including aptamer- and antibody-based assays, are also summarized. Advances in protein and small-molecule probes as well as MIP-based sensors are discussed with emphasis on sensitivity, selectivity, and potential for multiplexed, non-invasive monitoring. Overall, these sensors provide crucial insights into the development of accurate, cost-effective, and stable biosensing approaches for L-lactate and LDH detection in diverse settings.

Received 20th February 2026
Accepted 8th June 2026

DOI: 10.1039/d6ay00304d

rsc.li/methods



## 1. Introduction

Lactate is a critical chiral metabolite present in both enantiomeric forms in many living organisms. In humans, L-lactate is the dominant form that could be used to assess the physiological conditions of individuals. During anaerobic respiration, pyruvate generated from glycolysis cannot undergo efficient oxidation, thus are shunted toward fermentation to generate lactate by lactate dehydrogenase (LDH). Since the majority of body lactate is produced by muscular tissues, lactate concentration is a key indicator for athletic performance.[1] Abnormal lactate concentration is also a biomarker for diagnosing various pathological conditions including kidney and liver diseases and cancer. Under the physiological pH of 7.4, lactic acid exists as its anionic form of lactate, a weak conjugate base that serves as a buffer to neutralize excess protons produced.[2,3] For a healthy adult, resting serum L-lactate concentration ranges from 0.5–2.2 mM but can elevate to 25 mM during intense exercises.[4–7] In other body fluids, L-lactate concentrations range from 16 to 30 mM in sweat,[8,9] and can exceed 100 mM after exercises,[10] 0.2 to 4.9 mM in saliva,[11,12] 0.5 to 1.0 mM in tears,[13] and 0.2 to 1.0 mM in urine (Table 1).[14] Thus, sensors for monitoring L-lactate need to cover a broad concentration range to fit specific analytical needs.

Because of the critical role of lactate in human physiology and pathology, its detection has significant importance in both commercial and clinical applications and has become a subject of intensive research. Enzyme-based methods have long been employed for lactate sensing, with lactate oxidases (LOx) and lactate dehydrogenases (LDH) being the two most widely used enzymes.[15–17] Both enzymes catalyze redox reactions in which electron transfer can be measured and correlated with lactate concentration. Since the resulting electrical current is directly proportional to the lactate concentration in a sample, enzyme-based electrochemical sensors have become the most common approach for lactate detection. LOx catalyzes the oxidation of L-lactate to pyruvate in the presence of oxygen. During this process, hydrogen peroxide ($H_2O_2$) is produced as a by-product, which is subsequently oxidized at the electrode surface to enable detection.

LDH is a ubiquitous tetrameric enzyme present in animals, plants, prokaryotes, and most human tissues. It requires $NAD^+$ as a cofactor to catalyze the conversion of L-lactate to pyruvate, concurrently reducing $NAD^+$ to NADH. The generated NADH can be electrochemically oxidized back to $NAD^+$, releasing

Table 1 Typical lactate levels in various body fluids

| Body fluids | [Lactate] (mM) | Ref. |
|---|---|---|
| Serum (resting) | 0.5–2.2 | 4–7 |
| Serum (exercise) | 25 | 4–7 |
| Sweat (rest) | 16–30 | 8 and 9 |
| Sweat (exercise) | >100 | 10 |
| Saliva | 0.2–4.9 | 11 and 12 |
| Tears | 0.5–1.0 | 13 |
| Urine | 0.2–1.0 | 14 |

*Department of Chemistry, Waterloo Institute for Nanotechnology, University of Waterloo, Waterloo, Ontario, N2L 3G1, Canada. E-mail: liujw@uwaterloo.ca*

Table 2 Comparison of sensing strategies for lactate and LDH

| Sensing strategy | Detection limits and ranges | Advantages | Limitations | Wearable sensors | Ref. |
|---|---|---|---|---|---|
| Aptamers | In the mM range for L-lactate detection. For LDH binding, $K_d$ can reach nM | High specificity, affinity; reproducibility; thermal stability; easy surface modification | Susceptible to nuclease degradation; performance varies in complex biofluids | Highly suitable, compatible with flexible electronics | 28–30 |
| Molecular probes | mM range for L-lactate | Rapid signal generation; simple assay formats; possible real-time monitoring | Limited selectivity in complex matrices; photobleaching; interference by background autofluorescence | Moderately suitable, mainly optical systems | 31–33 |
| MIPs | pM to mM range | Excellent stability; low cost; long shelf life; resistant to harsh conditions | Template leakage; lower affinity than biological receptors | Promising for wearable applications | 34–36 |
| Antibody | Not suitable for lactate. LDH: nM range | Exceptional selectivity and well-established biorecognition platform | High production cost; limited thermal stability; irreversible denaturation possible; batch-to-batch variability | Limited by stability, denaturation and slow kinetics | 37 and 38 |

electrons that are detected by the electrode. Compared with traditional laboratory techniques such as HPLC, enzyme-based sensors enable the development of portable and user-friendly devices. Beyond enzymatic approaches, considerable effort has also been directed toward inorganic nanomaterial-based electrochemical sensors,[18] and lactate detection often incorporate nickel-based materials.[19–22] As enzyme-based methods have been extensively reviewed,[23–25] those contents will not be repeated here.

Despite their advantages and extensive study, enzyme-based sensors face several intrinsic limitations. First, enzymes depend on well-defined tertiary and quaternary structures for catalytic activity, restricting their operation to narrow ranges of temperature, pH, and ionic strength. As physiological conditions fluctuate, these sensors are susceptible to denaturation, leading to reduced accuracy. Second, enzyme-based sensors generally have shorter shelf lives than synthetic alternatives, particularly at ambient temperatures; enzymes often require storage at −80 °C to prevent degradation, posing challenges for long-term monitoring. Finally, the extraction, purification, and immobilization of active proteins are costly, limiting the affordability and scalability of enzyme-based systems.

To address these limitations, an alternative class of detection methods employs affinity ligands, such as antibodies, aptamers, molecular probes, and molecularly imprinted polymers. Rather than relying on catalytic reactions, these sensors detect target analytes through specific binding interactions. Owing to their ease of modification and relatively low cost, affinity ligand-based sensors are increasingly attractive for the development of portable and continuous monitoring devices for various metabolites. With the recent emergence of lactate-binding aptamers,[26,27] affinity ligand-based detection is gaining growing attention as a promising research direction.

In addition to lactate, lactate dehydrogenase (LDH) is an important analytical target. Studies have shown that LDH levels correlate with lactate under certain pathological conditions, making LDH detection a potential indirect approach for lactate monitoring. Accordingly, this review also covers LDH detection strategies. Given the clinical significance of accurately and efficiently monitoring L-lactate and LDH in various body fluids across both clinical and athletic settings, substantial research has focused on affinity-based biosensors. Here, we evaluate the strengths and limitations of different platforms for L-lactate and LDH detection, including those based on aptamers, proteins, small molecule probes, and molecularly imprinted polymer (MIPs) as shown in Table 2.

## 2. Aptamer-based biosensors

Aptamers are single-stranded nucleic acids that can selectively bind to target molecules.[39–42] Aptamers were first reported in 1990 using a combinatorial biology method called systematic evolution of ligands by exponential enrichment (SELEX).[43,44] Later, naturally occurring aptamers known as riboswitches were discovered, which were found in the untranslated regions of mRNA in many bacterial cells.[43] While riboswitches binding to dozens of metabolites have been reported, none of them is for lactate. Compared with antibodies, aptamers offer several advantages, including smaller size and molecular weight, low immunogenicity, and greater structural stability across a wide range of temperatures, ionic strengths, and pH conditions.[45,46] Moreover, aptamers are particularly well suited for binding small molecules, whereas antibodies are often less effective for metabolite detection.[47] Aptamers function through rapid conformational changes into defined secondary structures upon target binding, enabling high specificity and programmability.[48,49] These properties make aptamers especially well-suited for detecting small metabolites such as lactate.

### 2.1. Lactate binding aptamers selected using L-lactate

The first L-lactate binding aptamers were reported by our group by the capture-SELEX method.[27] The 10 most abundant

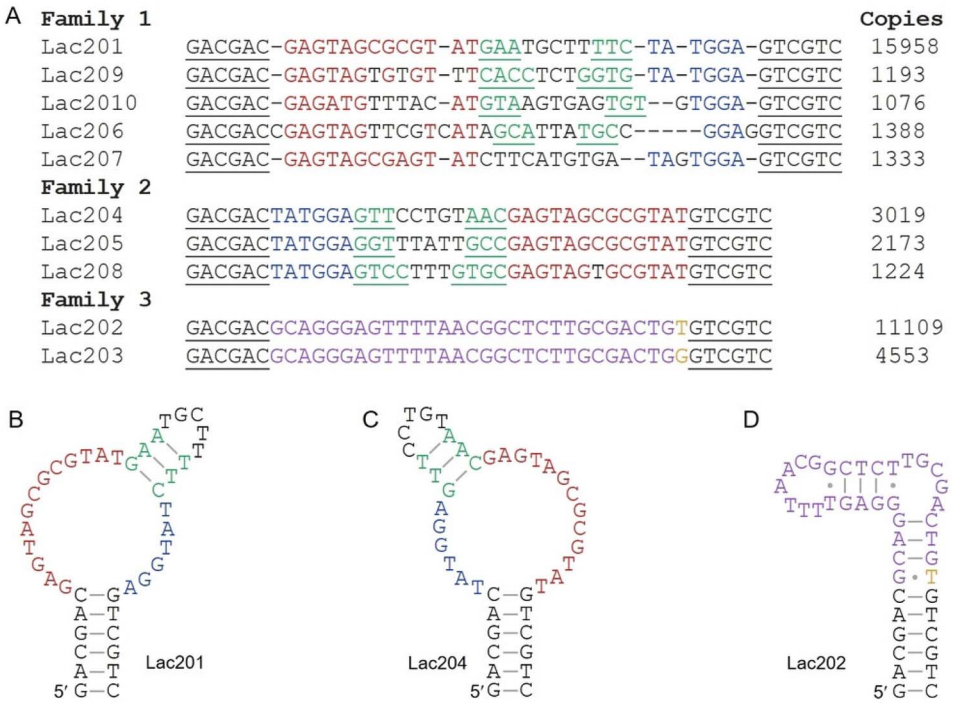


Fig. 1 Secondary structures of L-lactate binding aptamers generated using SELEX. (A) Sequence alignment of the most abundant sequences in the library. The secondary structures of the (B) Lac 201, (C) Lac 204, and (D) Lac 202 aptamers. Adapted from ref. 27 with permission from Wiley, *Angewandte Chemie International Edition,* 2023, **62**, e202212879, copyright 2023.

sequences in the library can be assigned to 3 families (Fig. 1A), and the secondary structures of these 3 families (Fig. 1B and D) were predicted by mFold (Fig. 1B and D).[50] Isothermal titration calorimetry (ITC) shows that the Lac201 aptamer has a dissociation constant ($K_d$) of 0.43 mM, which falls within the physiological lactate range at rest. Notably, it retains binding

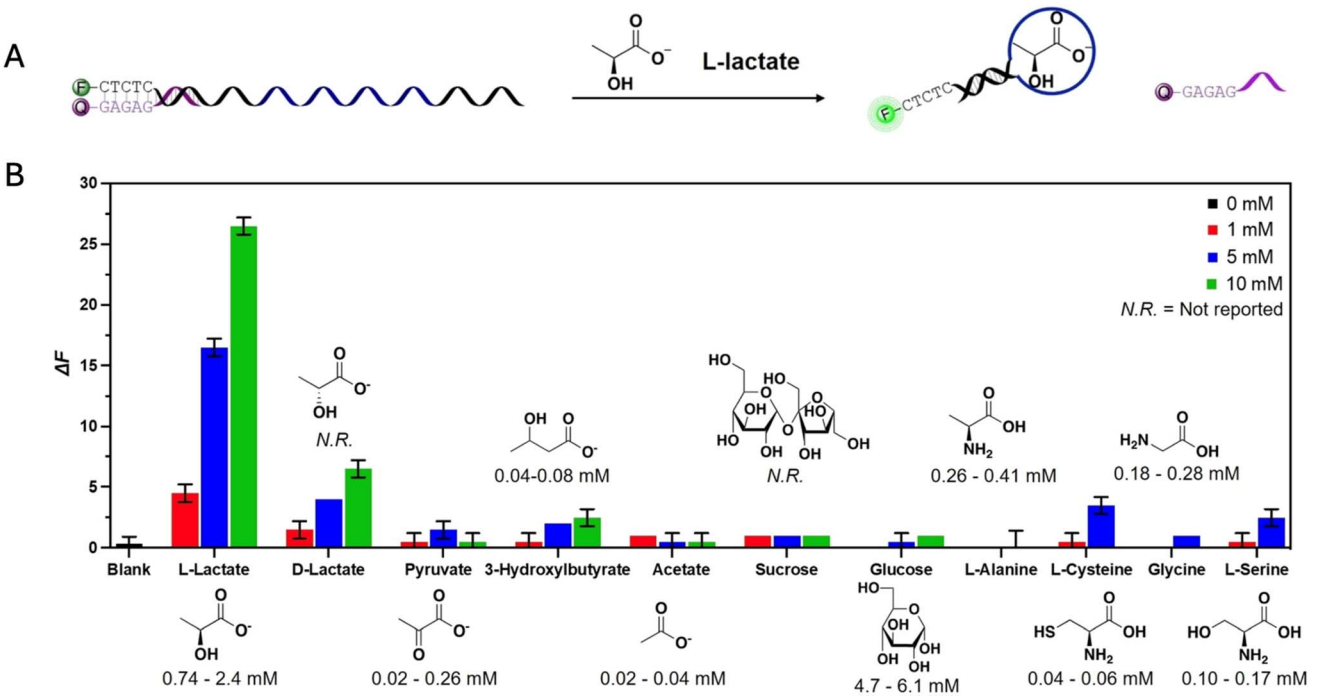


Fig. 2 (A) A schematic demonstration of the fluorescent biosensing mechanism for lactate detecting aptamers. (B) Selectivity of Lac 201. It is demonstrated that out of the common interferents tested, the aptamer showed high selectivity towards L-lactate. Adapted from ref. 27 with permission from Wiley, *Angewandte Chemie International Edition,* 2023, **62**, e202212879, copyright 2023.

performance even in 90% serum, highlighting its potential for *in vivo* lactate monitoring.

Sensing of lactate was first demonstrated using a DNA strand displacement assay by extending the 5′-end of the aptamer with 5 nucleotides and labeling it with a 5′-FAM fluorophore (Fig. 2A). This FAM-labeled aptamer was then hybridised with a quencher-labeled 12-mer DNA, where upon analyte binding of the aptamers, the quencher strand was displaced leading to increased fluorescent intensity. This sensor achieved a limit of detection (LOD) of 0.55 mM. In addition, the Lac201 aptamer was 7-fold more selective for L-lactate than D-lactate (Fig. 2B).

This L-lactate sensing aptamer has also been examined for potential application. Bakhshandeh *et al.*[51] constructed a wearable aptamer-based sensor using microneedle to electrochemically detect biomarkers including lactate and glucose in the interstitial fluid of animals (Fig. 3A). First, hyaluronic acid (HA) was modified with methacrylic anhydride (MA) to produce highly and lightly crosslinked methacrylated HA (HC-MeHA and LC-MeHA). HC-MeHA was then used to mold the hydrogel microneedles, while LC-MeHA served as a thin adhesive layer between the electrode and the microneedle (Fig. 3B). The Lac201 aptamer was tagged with a methylene blue (MB) as a redox reporter and attached to a gold working electrode. Upon binding to lactate, the aptamer undergoes a conformational change, bringing the MB closer to the gold surface, resulting in increased electron transfer (Fig. 3C). The

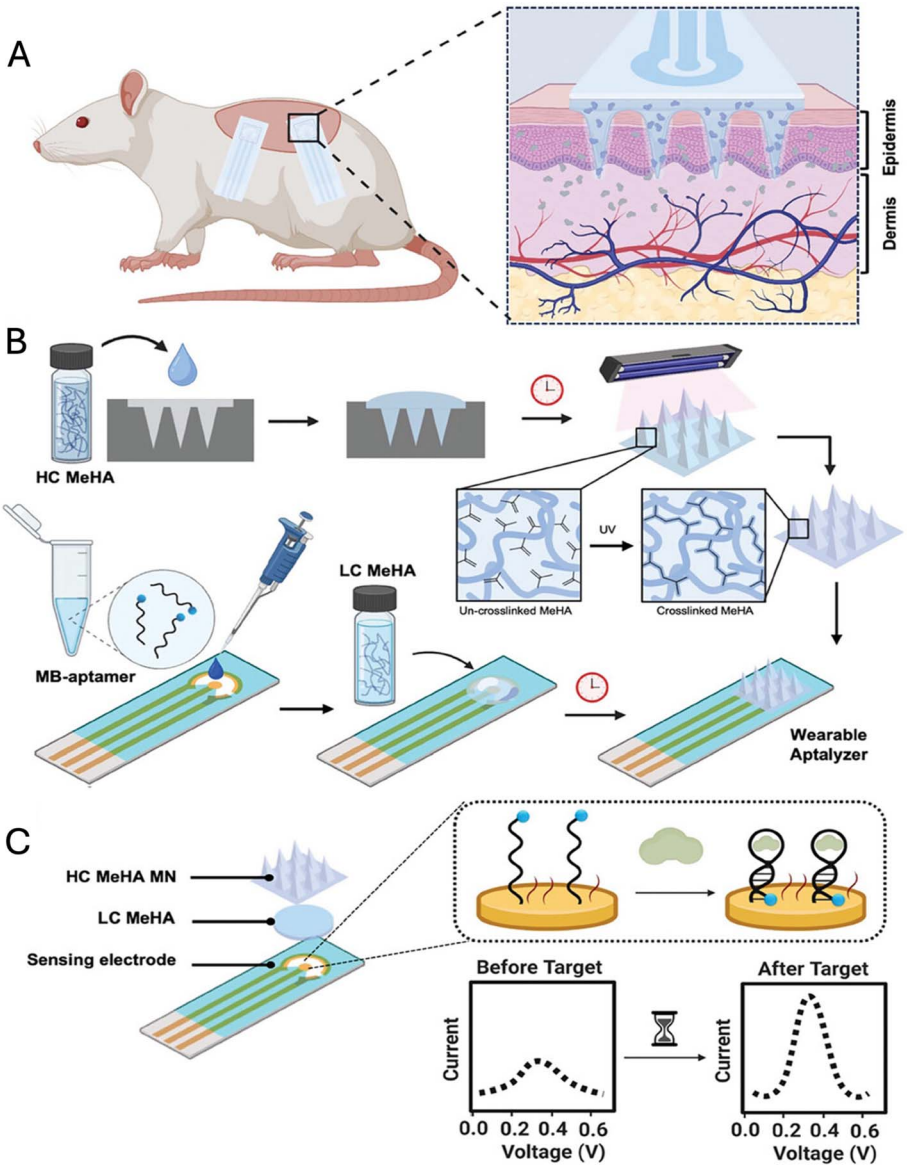


Fig. 3 (A) Schematic demonstration of the wearable aptamer-based sensor using microneedles on mice. (B) Procedures for the construction of hydrogel microneedles and the integration of aptamers into the sensor. (C) Mechanism of analyte detection through conformational change in DNA secondary structure and detection of induced voltage change. Adapted from ref. 51 with permission from Wiley, *Advanced Materials*, 2024, **36**, 2313743, copyright 2024.

A

| Names | Previous names | Family 1 Sequence (5′ to 3′) | Abundance |
|---|---|---|---|
| D-Lac1101 | Lac201 | GACGACGAGTAGCGCGTATGAATGCTTTTTCTATGGAGTCGTC | 25.75% |
| D-Lac1104 | Lac207 | GACGACGAGTAGCGAGTATCTTCATGTGATAGTGGAGTCGTC | 0.23% |
| D-Lac1106 | Lac209 | GACGACGAGTAGTGTGTTTCACCTCTGGTGTATGGAGTCGTC | 0.07% |
| D-Lac1107 | Lac2053 | GACGACGAGTAGTGAGTACAACTWGCAGTTTGTGGAGTCGTC | 0.04% |
| D-Lac1111 | Lac2021 | GACGACGAGTAGCGTGTATATTCGGAGAAGTATGGAGTCGTC | > 0.01% |

| Names | Previous names | Family 2 Sequence (5′ to 3′) | Abundance |
|---|---|---|---|
| D-Lac1102 | Lac205 | GACGACTATGGAGGTTTATTGCCGAGTAGCGCGTATGTCGTC | 18.62% |
| D-Lac1108 | N/A | GACGACCTATGGAGCACATTGCGAGTAGCGTGTATGGTCGTC | 0.02% |
| D-Lac1112 | N/A | GACGACTATGGAGGTTTATCGCTGAGTAGCGCGCATGTCGCC | > 0.01% |
| D-Lac1124 | Lac2011 | GACGACTATGGAAGAGTGTGTCTGAGTAGCGTGTATGTCGTC | > 0.01% |

| Names | Previous names | Family 3 Sequence (5′ to 3′) | Abundance |
|---|---|---|---|
| D-Lac1103 | Lac2059 | GACGACATTCACACAGGTGGACATTTAGGAGGTGATGTCGTC | 16.81 % |
| D-Lac1110 | N/A | GACGACCTTCACACAGGGGGACATGGAGGAGGTGAGGTCGGC | 0.02% |
| D-Lac1113 | N/A | GACGACATGCACACAGGGGGACAGTGAGGAGGTGATGTCGGM | > 0.01% |
| D-Lac1137 | N/A | GACGACAGTCACACAGGCGGACAGTRAGGAGGTGAGGTCGGC | > 0.01% |
| D-Lac1141 | Lac2079 | GACGACMTTCACACAGGTGGACATTTAGGAGGTGAKGTCGTC | > 0.01% |
| D-Lac1144 | N/A | GACGACAGGCACACAGGGGGACATGCAGGAGGTGAGGTCGGC | > 0.01% |

B

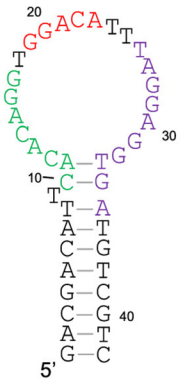


D-Lac1103

Fig. 4 (A). L-lactate binding aptamer sequences and categorization into 3 families. (B) Secondary structure of the D-Lac1103 aptamer from Family 3. Adapted from ref. 26 with permission from American Chemical Society, *Analytical Chemistry*, 2026, **98**, 7515–7523, copyright 2026.

sensor has a LOD of 1.04 mM. The sensor was tested on a range of common interferents in ISF including sugars, amino acids, and other small molecules, showing high selectivity towards lactate. Recently, the lactate aptamer was also used to crosslink hydrogels and such gels can in turn be sensitive to lactate.[52]

### 2.2. Searching for D-lactate binding aptamers yielding a better L-lactate aptamer

The identification of L-lactate aptamers also motivated the search for D-lactate-binding aptamers. D-lactate is primarily generated through bacterial metabolism. Humans have limited capacity to metabolize D-lactate. In healthy individuals, plasma D-lactate concentrations typically range from 0.006 to 0.25 mM.[53] Elevated D-lactate levels are generally associated with pathological conditions. For instance, D-lactate acidosis is a serious complication in patients with short bowel syndrome, where excessive production of D-lactate by the gut microbiota leads to plasma concentrations exceeding ~3 mM. This condition is often accompanied by neurological symptoms, including confusion and ataxia.[54,55]

Using 100 mM D-lactate as target for aptamer selection, we also obtained 3 families of sequences (Fig. 4A). Families 1 and 2 closely resembled that of the L-lactate binding aptamers mentioned above. Therefore, Lac1103 from family 3 was examined more closely (Fig. 4B). Interestingly, Lac1103 still exerted higher binding affinity towards L-lactate than D-lactate. For example, using the fluorescence strand-displacement assay, an apparent $K_d$ of 0.46 mM for L-lactate and 2.5 mM for D-lactate was obtained. ITC showed a $K_d$ of 0.11 mM for L-lactate. While we failed to obtain an aptamer with higher affinity to D-lactate, we obtained a better L-lactate aptamer that can be used for the detection of L-lactate in lower concentrations. This observation suggests that DNA aptamers might have intrinsic preferences to certain chirality.

## 3. Lactate binding proteins for lactate detection

While high-quality antibodies for lactate are not known, some naturally occurring proteins can selectively bind to lactate. Nasu *et al.*[32] reported a genetically encoded fluorescent lactate probe that is spectrally and spatially multiplexed. By respectively linking green (cpGFP) and red fluorescent proteins (cpmApple) to the lactate-binding periplasmic protein TTHA0766 endogenous to *Thermus thermophilus*, this detection probe system was able to simultaneously and orthogonally detect extracellular and intracellular lactate molecules, respectively (Fig. 5).

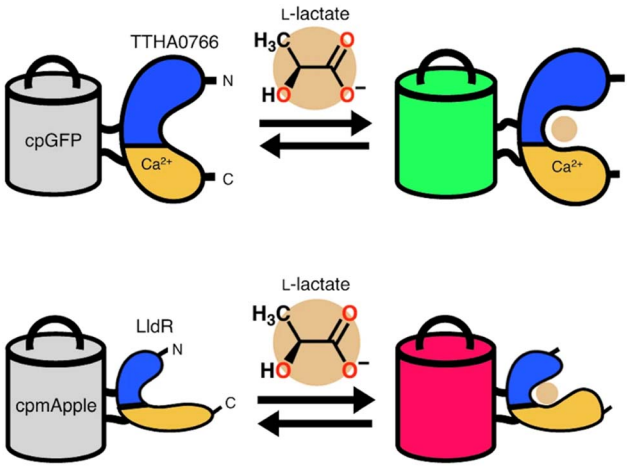


Fig. 5 Protein fluorescent probe for lactate detection both intracellularly and extracellularly. The lactate binding proteins and the fluorescent proteins are connected by peptide linkers. Adapted from ref. 32 with permission from Springer Nature, *Nature Communications*, 2023, **14**, 6598, copyright 2023.

Directed evolution was conducted on the 2 types of sensors for greater change in fluorescent intensity ($\Delta F/F$) upon lactate treatment. The optimal GFP-linked sensor was named eLACCO2.1, while the optimal red fluorescent protein linked sensor was named R-iLACCO1 (Fig. 5).

Results of the detection system showed that eLACCO2.1, the second-generation green fluorescent L-lactate biosensor modified from their previous work,[56] showed a $\Delta F/F$ of 14 as purified protein when treated with 10 mM of L-lactate. The red fluorescent L-lactate sensor R-iLACCO1, on the other hand, showed a $\Delta F/F$ of 20. In terms of affinity, eLACCO2.1 had an *in situ* apparent $K_d$ of 580 μM and $Ca^{2+}$ dependent fluorescence. The sensor eLACCO2.1 had an *in situ* apparent $K_d$ of 680 μM. These affinities are comparable to the binding of L-lactate by aptamers, suggesting that proteins and DNA are comparable for molecular recognition of this target. Recently, a red fluorescence version of this sensor was also developed.[57]

Chang *et al.*[31] and Li *et al.*[58] developed a sensor call FiLa to detect the spatiotemporal landscape of cellular lactate metabolism. FiLa was developed by linking a fluorescent protein to the lactate-binding protein LldR. LldR is a transcriptional regulator found in *E. coli* and other bacteria that binds to DNA promoter regions in the absence of lactate. Upon lactate binding, LldR undergoes a conformational change and dissociates from the promoter. This property has been leveraged to create highly sensitive lactate sensing probes. Fluorescent proteins of different colors have also been incorporated for specific applications; for example, red fluorescent proteins, with emission wavelengths of ~600 to 700 nm, enable deeper tissue penetration compared with green or blue fluorescence, making them advantageous for *in vivo* lactate imaging.

## 4. Small molecular probe-based biosensors

A molecular probe is a molecule or complex, either synthetic or naturally occurring, that can be used to detect other molecules or structures through binding interactions. Compared to aptamers and proteins, small molecule probes can be designed for cell penetration and other functions. In addition, they are often more stable compared to biopolymers.

A recent publication by Wojcieszek *et al.*[59] illustrated a printed lactate sensor based on a Zr(IV)-porphyrin ionophore. Specifically, Zr-tetraphenylporphyrin (Zr-TPP) and Zr-octaethylporphyrin (Zr-OEP) were mixed with polyurethane, lipophilic additives, and plasticizer to prepare the ionic-selective electrode (ISE) membranes. The sensor material mixture was then drop-casted on the surface of a graphene screen-printed electrode, forming a non-catalytic, potentiometric lactate sensor. Moreover, the Zr-porphyrin membranes were prepared in 2 variants: PU plasticized with polar *o*-NPOE, containing anionic ($TFPB^-$) additives, and PU plasticized with non-polar DOS, containing cationic ($TDMA^+$) additives. The $Zr^{4+}$ center in the porphyrin structure exerts high affinity for the carboxylate group. As lactate from the sample diffuses into the ISE membrane, a stable coordination complex between lactate and Zr-porphyrin will be formed (Fig. 6A). Such binding alters the ionic activity and charge distribution at the membrane, generating a measurable change in membrane potential. Out of these sensors, the Zr-TPP plasticized with DOS, containing cationic $TDMA^+$ additives demonstrated the best sensitivity and selectivity towards lactate with a sensitivity of −76.6 mV $dec^{-1}$ and a linear range from $10^{-4}$ M to $10^{-1}$ M. To evaluate selectivity, the researchers tested common anions present in human

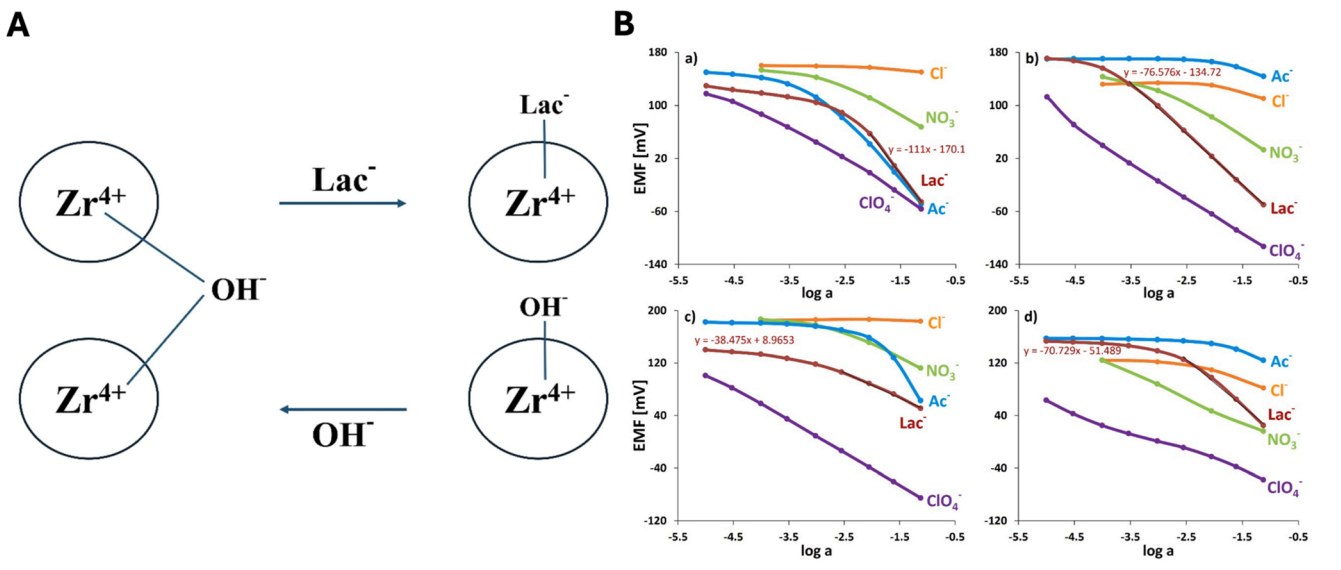


Fig. 6 (A) Schematic representation of Zr-porphyrin dimer–monomer equilibrium and its changes caused by increasing lactate concentration. (B) Testing various anions for classical electrodes with membranes: (a) Zr-TPP/PU/o-NPOE/KTFPB; (b) Zr-TPP/PU/DOS/TDMACl; (c) Zr-OEP/PU/o-NPOE/KTFPB; (d) Zr-OEP/PU/DOS/TDMACl. Measurements were performed in MES buffer solution, pH 5.5. Adapted from ref. 59 with permission from Elsevier, *Sensors and Actuators B: Chemical*, 2024, **421**, 136475, copyright 2024.

sweat, including chloride, nitrate, acetate, lactate, and perchlorate (Fig. 6B). Although Zr-TPP exhibited preferential response to lactate, perchlorate emerged as a notable interferent, and overall selectivity was limited compared with other reported lactate sensors. This outcome is expected given the less specific binding mechanism. Overall, while the sensor demonstrates some degree of sensitivity and selectivity toward lactate, there is still room for further improvement.

# 5. MIP-based sensors

Molecularly imprinted polymers (MIPs) are polymers synthesized in the presence of a template molecule, where a cavity with the shape of the imprinted target is formed in the polymer matrix.[60] MIPs are cheaper and higher in stability compared to antibodies, although the binding affinity and specificity of MIPs is usually lower. Different types of MIP-based biosensors such as optical and luminescent sensors.[35,61–65] Lactate represents a very challenging target molecule for MIPs since it has very low binding epitopes.

## 5.1. MIPs for lactate

For making MIP-based lactate biosensors, positively charged monomers are often used since lactate is negatively charged. As indicated in Table 3, positively charged 3-APTES is a commonly used functional monomer for electrochemical lactate sensors. Another type of monomer contains boronic acid derivatives such as 3-APBA and 5-indolylboronic acid, which can form reversible bonds with molecules that have *cis*-diols or α-hydroxycarboxyl group. Fig. 7 shows the structures of various functional monomers used for imprinting lactate, and mixing a few different monomers, even better binding performance could potentially be achieved.

## 5.2. MIP-based electrochemical sensors for lactate

Dykstra *et al.*[36] proposed a reagent-free MIP-based detector to monitor sweat lactate. Traditional MIP-based electrochemical sensors require external redox probes for detecting MIP-analyte binding. Their sensor, instead, utilizes Prussian Blue (PB), a widely used electron-transfer mediator for enzymatic biosensors,[74,75] and incorporated an internal layer of PB nanoparticles using electrodeposition in acidic environment. On top, a 3-APBA and pyrrole MIP layer was synthesized in neutral environment for lactate detection. When tested in 0.1 KCl (pH 6.5), the LOD is 0.20 mM, while in artificial sweat (pH 6.5), the LOD is 0.62 mM. Furthermore, it is shown that the sensor has a shelf life of 10 months in ambient environment, making it a promising candidate for long-term monitoring of lactate levels.

Chen *et al.*[76] integrated large-scale flexible MIP-based sensors into textile fabrics for long-term sweat lactate monitoring. By constructing electrodes from carbon nanotube fibers, the design improved the interface between the fibers and MIP

Table 3 Summary of recent publications on MIP-based detection for lactate

| Sensor | LOD | Detection method | Functional monomers | Linear detection range | Ref. |
|---|---|---|---|---|---|
| PtNPs/Pt@MIP | 1.09 mM | Electrochemical | Pyrrole | 5–30 mM | 66 |
| ZIF-8@ZnQ@MIP-GCE | 29.9 fM | Electrochemical | 4-ABA | 1.1–1.0 pM | 67 |
| MIP | 0.162 mM | Electrochemical | MAA | 1.1–1.7 mM | 68 |
| MIP/Ag-AuNPs | 0.03 μM | Electrochemical | — | 1–220 μM | 69 |
| PANI-co-PBA@ AuNP | 13 mM | Electrochemical | 3-APBA | 4.5–56 mM | 70 |
| MIP | 0.2 mM | Electrochemical | 3-APBA & pyrrole | 1–35 mM | 36 |
| MIP@PIn-BAc/ZnO | 3.38 mM | Optical | 3-APTES & 5-indolylboronic acid | 0–30 mM | 71 |
| MIP-TES | — | Triboelectric | 3-APBA | 0–20 mM | 72 |
| MIP-AgNWs | 0.22 μM | Electrochemical | 3-APBA | — | 73 |

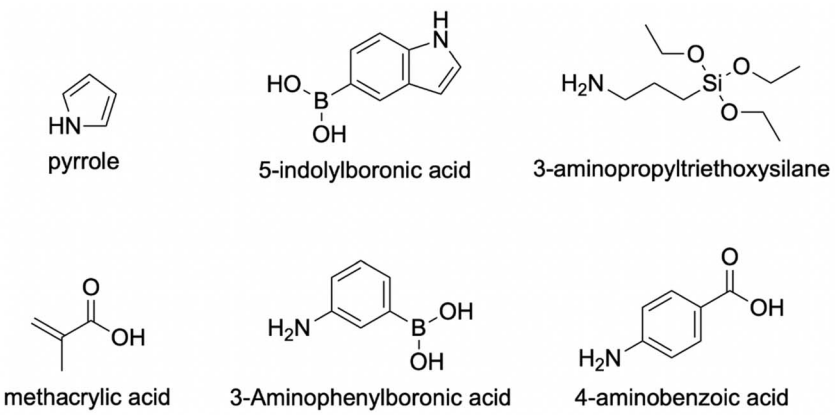


Fig. 7 The commonly used functional monomers in MIP-based sensors for lactate detection.

layers, enhancing both reusability and analyte diffusion for more effective biomarker detection. The fabric-based biosensor demonstrated stable, repeated *in situ* lactate measurements over more than 400 cycles. In terms of performance, it exhibited a wide detection range from 10 μM to 25 mM.

### 5.3. MIP-based optical sensors for lactate

While most MIP-based sensors for lactate detection relied on electrochemistry, a recent publication by Wusiman *et al.*[71] demonstrated the first portable MIP fluorescent sensor for lactate detection. In this publication, the ZnO QDs were used as a quantifiable fluorescent source to detect lactate binding. The researchers did a comparison between two sensing materials using two functional monomers: 3-APTES and 5-indolylboronic acid. The ZnO@APTES-MIP was prepared in a one-step procedure by mixing APTES dispersed QDs with APTES, lactic acid, TEOS and additional ingredients at pH 7.0, whereas the MIP@PIn-BAC was prepared in a two-step procedure (Fig. 8A). The NIP versions of these materials were also prepared without the addition of lactate, and the sensing materials were subsequently coated onto quartz chips by spin coating. Because of the thin film coating, simple optical detectors can be used.

The sensors were tested on lactate, ascorbic acid, uric acid, and glucose in DI water and PBS. Results indicated that in the PBS, the MIP@PIn-BAC sensor has a detection range of 0–30 mM of lactate. The MIP@PIn-BAc/ZnO exerted much better selectivity towards lactate, while ZnO@APTES-MIP cannot distinguish between lactate and other tested molecules. Although more cost-effective and more stable, MIP-based biosensors also face several limitations such as lower binding affinity and specificity compared to antibodies.

## 6. Sensors for LDH detection

Under normal physiological conditions, LDH is primarily localized within tissues, with serum levels typically ranging from 140–280 U $L^{-1}$ in adults, 150–300 U $L^{-1}$ in adolescents, and 160–450 U $L^{-1}$ in infants. Serum LDH levels exceeding 500 U $L^{-1}$ generally indicate tissue damage (cytolysis) and the release of LDH into circulation. While elevated lactate levels do not always correspond to increased LDH (*e.g.*, during intense exercise), elevated LDH is commonly associated with pathological conditions.[77] This is often accompanied by increased lactate levels (>2.0 mM), resulting either from impaired tissue oxygenation (type A lactic acidosis), such as in hemorrhage or hypoperfusion, or from enhanced lactate production under normoxic conditions (type B lactic acidosis) due to metabolic or organ dysfunction.[78–80] Given the correlation between LDH and lactate in certain pathological states,[81,82] and the role of LDH in lactate metabolism, this section reviews affinity-based sensors for LDH following the discussion of lactate detection.

### 6.1. LDH binding aptamers and their clinical applications

Over the years, several publications have addressed the development of aptamer-based sensors for LDH detection. A primary example is the development of aptamer-based diagnosis of the

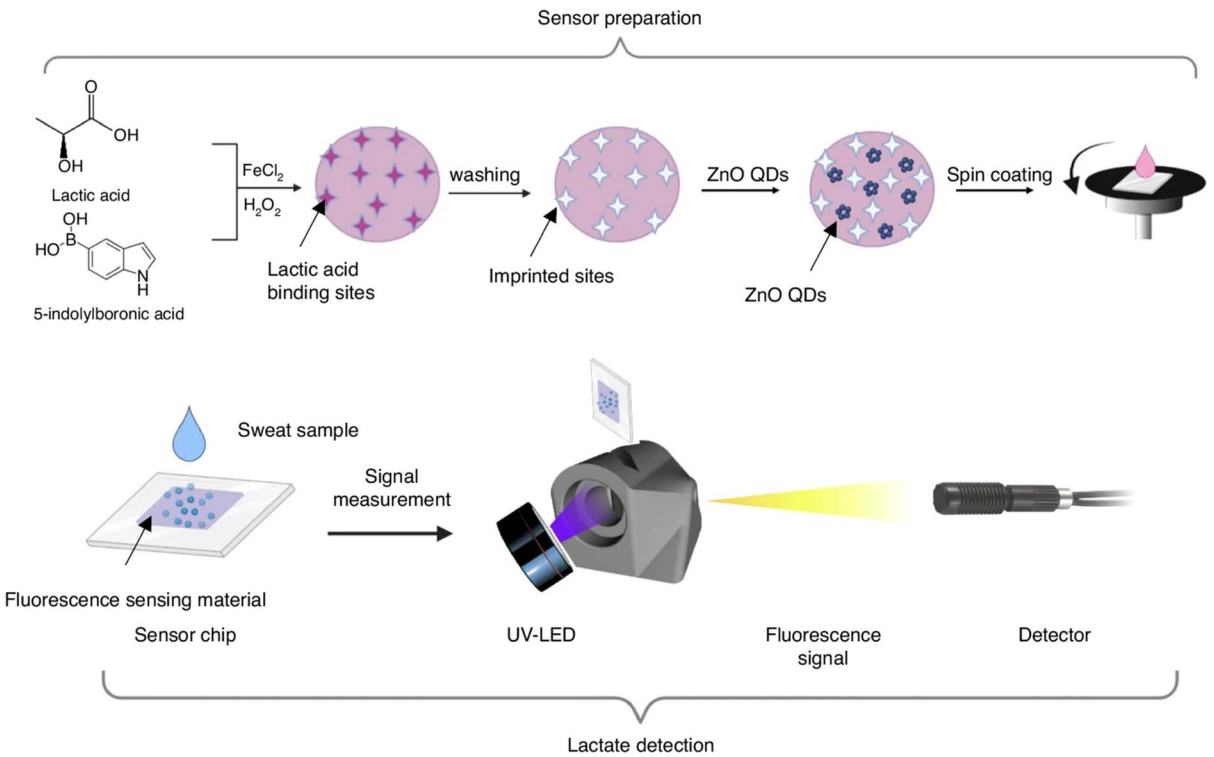


Fig. 8 Schematic demonstration of the first portable MIP-based biosensor for lactate monitoring. The detection mechanism uses ZnO QDs as quantifiable fluorescence signals to detect binding.[71] Adapted from ref. 71 with permission from Springer Nature, *Microsystems & Nanoengineering*, 2024, **10**, 175, copyright 2024.

malaria biomarker. The Tanner lab[83] obtained an aptamer named "2008s" that exerted high specificity toward *Plasmodium falciparum* LDH (PfLDH) (Fig. 9A). They screened a library containing a random 35 nt region using affinity chromatography for PfLDH binding. A counter-selection step was introduced to eliminate aptamers binding human LDHA1 and LDHB. The 2008s aptamer demonstrated excellent affinity towards PfLDH with a $K_d$ in the range of 42 – 59 nM while showing negligible binding to human LDHs. Crystal structures of the aptamer–protein complex revealed that 2 aptamer molecules bind symmetrically to the PfLDH tetramer, spanning 2 subunits each. The aptamers specifically interact with the PfLDH substrate specificity loop (residue 102–108) which is a region absent in human LDHs (Fig. 9B). Subsequently, the same group further examined the specificity of the 2008s aptamer towards PfLDH and compared the aptamer with a previously discovered pL1 aptamer[84,85] that could bind to both pf and PvLDH using aptamer-tethered enzyme capture (APTEC) assay and enzyme-link oligonucleotide assay (ELONA). In this publication, the researchers applied the two aptamers to patient blood samples and compared them under actual clinical conditions. The researchers demonstrated the potential of developing fast and cost-effective aptamer-based malaria diagnosis methods to distinguish between PfLDH and *Plasmodium vivax* LDH (PvLDH).[86]

Guo *et al.*[28] used four libraries containing random regions from 30 to 60 nt to select aptamers for human LDH, and LDH was immobilized on magnetic beads for positive selection. In the end, four aptamers (LDH7-1, LDH7-9, LDH8-2, and LDH9-1) showed $K_d$ values below 25 nM, indicating strong binding affinity. Selectivity was tested against human serum, serum alpha-fetoprotein (AFP), and bovine serum albumin (BSA), and the candidate aptamers showed high specificity towards LDH.

Kim and Choi reported an enzyme-linked aptamer-based sandwich assay (ELISA) for PfLDH detection based on the 2008s aptamer.[87] The assay involved immobilizing biotinylated aptamers in a streptavidin coated well, where the aptamers would bind to PfLDH. HRP conjugated aptamers were

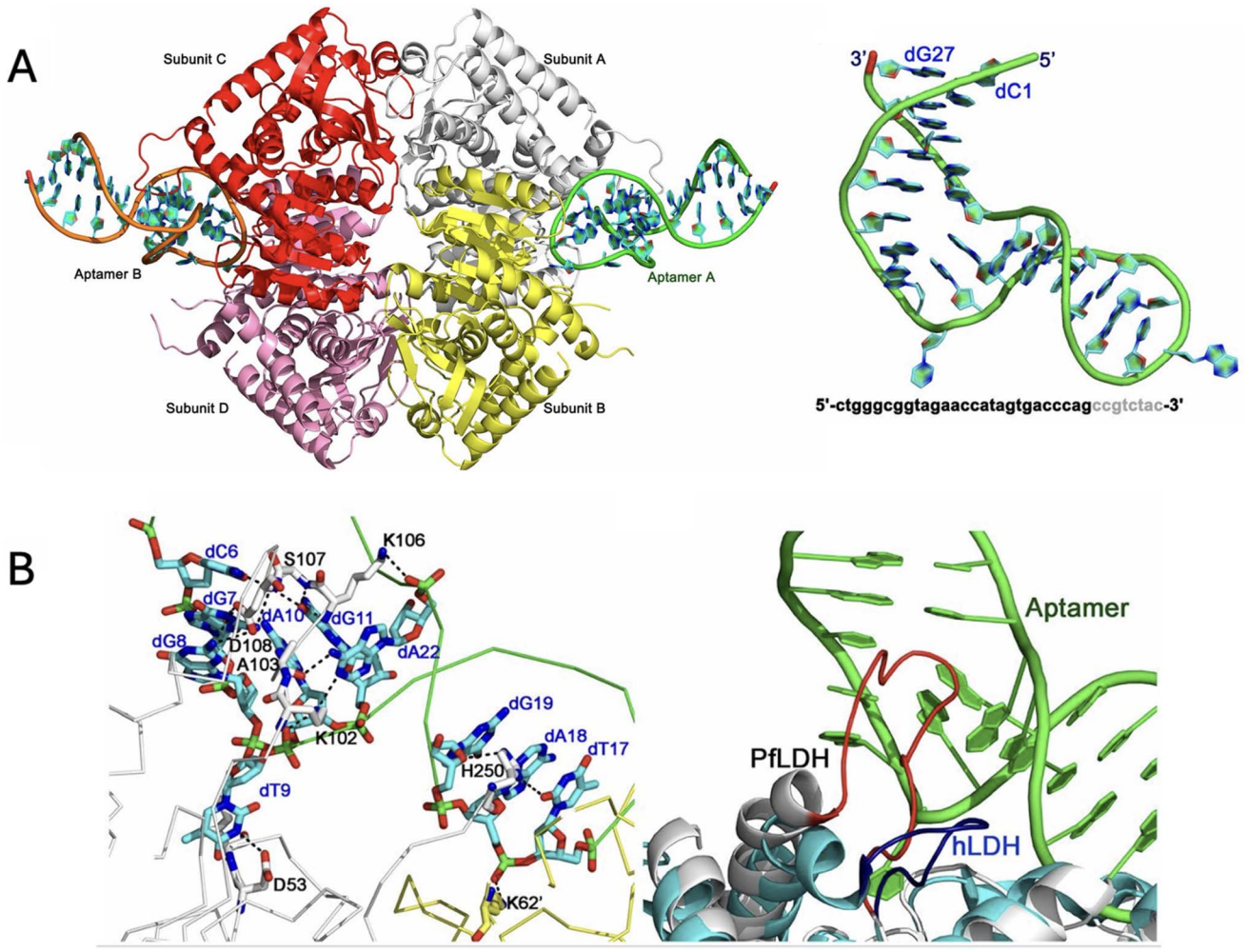


Fig. 9 (A) Crystal structure of PfLDH binding aptamer- PfLDH complex. (B) Zoom-in view of the interaction between PfLDH substrate specific loop and the aptamer. Adapted from ref. 83 with permission from National Academy of Sciences, *Proceedings of the National Academy of Sciences*, 2013, **110**, 15967–15972, copyright 2013.

subsequently added to the wells. After washing away unbound aptamers, TMB substrate was added to the mixture, and colour change could be measured to quantify enzyme concentration. When tested on blood samples, the LOD of the sensor was 34.9 ng $mL^{-1}$ with good selectivity.

In 2025, Yuan *et al.*[88] developed a novel electrochemical aptamer sensor that can quantify the serum concentration of PfLDH in a single step and a few minutes. The researchers re-engineered two aptamers specific for PfLDH binding: "2008s" and "P11" (ref. 89) to maximize their binding-induced conformational change and consequently maximizing signal transduction. Variants were generated by shortening them from the 5′ or 3′ ends in increments of approximately 5 bases, which destabilized the secondary structures to induce a greater conformational change during target binding. After optical (a fluorophore-quencher pair) and electrochemical characterization of these aptamers, sensors were constructed by respectively immobilizing these aptamers onto electrodes. The P11-30 variant showed the best performance for rapid and specific detection of PfLDH with an apparent $K_d$ of 161 ± 47 nM.

### 6.2. Antibody-based sensor for LDH detection

Sousa *et al.*[37] described a polyclonal antibody-based sandwich ELISA to detect pvLDH in clinical blood samples. To obtain the antibodies, mice and rabbit were immunized with 2 segments of pvLDH protein (pvLDH1-43 and pvLDH35-305) obtained using recombinant protein expression. Following inoculation, total serum was obtained, and IgG was purified. For detection, rabbit polyclonal antibody anti-pvLDH 1-43aa was immobilized, and upon sample addition, pvLDH was attached to the antibody. After washing, 2 types of primary mouse antibodies (anti-pvLDH 1-43aa and anti-pvLDH 35-305aa) were added respectively, following by HRP conjugated secondary antibodies (anti-mouse IgG antibodies). Both mouse antibodies showed selectivity towards pvLDH and could not detect pfLDH in human clinical blood samples.

In 2025, Banguera-Ordoñez *et al.*[90] developed a lateral flow immunoassay (LFIA) integrated with smartphone for rapid, sensitive, and specific detection of serum LDH concentration to monitor tissue damage and diseases. The researchers first obtained high affinity monoclonal antibodies for LDH with a $K_d$ of 5 nM. To enhance the sensitivity of LFIA, carbon nanoparticles (CNPs) were used as signal transducers instead of the conventional AuNPs. The anti-LDH antibodies were covalently coupled to the CNPs and integrated into the LFIA test strip. A smartphone-based system was developed to read and analyze the LFIA results through capturing the images of the test strip and quantifying LDH levels. Result demonstrated that the CNP-based LFIA showed a 55-fold improvement in sensitivity compared to the conventional AuNP-based LFIA, achieving a detection limit of 1.5 ng $mL^{-1}$. For visual detection limit, the CNP-based LFIA (2.4 ng $mL^{-1}$) was 7.8 times lower than AuNPs (18.8 ng $mL^{-1}$).

Both aptamer and antibody-based sensors for LDH can achieve binding affinity in the nM region as well as high selectivity towards LDH. Despite both detection systems rely on binding to specific regions or epitopes of the enzyme, aptamer-based sensors appear to have the advantage of ease of modification.

## 7. Conclusion and future directions

L-lactate is a key metabolite and biomarker essential for maintaining physiological homeostasis, making efficient, accurate, and cost-effective detection methods critically important. Although enzyme-based sensors are widely used, they typically rely on detecting oxidation byproducts (*e.g.*, hydrogen peroxide or NADH), which can be susceptible to interference. Additionally, such sensors face limitations including short shelf life and challenges in enzyme purification and stability due to structural complexity. This review focuses on affinity-based sensors for direct L-lactate detection. While antibody-based sensors are commonly used for macromolecules, they are not available for lactate; however, given the correlation between lactate and LDH, antibody-based LDH detection is briefly discussed. We highlight the first L-lactate-binding aptamer discovered by our group. Other affinity probes discussed include lactate-binding proteins, as well as molecular probes based on metal coordination chemistry and MIPs.

Affinity-based sensors are not without limitations. Compared with enzyme-based systems, they may exhibit weaker binding affinities for small molecules and often struggle to achieve similarly low detection limits. In particular, enzymes have catalytic turnovers and thus can easily achieve amplified detection. In complex matrices such as human serum, nonspecific interference can further compromise sensor performance. Nevertheless, continued research is expected to address these challenges and advance the development of more robust and sensitive affinity-based detection platforms.

Given the current developments, a few future directions are possible. First, a horizontal comparison among the above-mentioned methods could be useful. When examining our aptamer-based sensor, MIP-based sensors, and molecular probes, most sensors mentioned have LODs and linear detection ranges in the mM concentrations with only a few exceptions having μM or even pM concentrations. This observation suggests the necessity of some standard reference methods to obtain more reliable experimental results. Second, aside from L-lactate, we have also discussed our findings on aptamers for simultaneous L and D-lactate detection. Aptamer-based sensors are especially promising because of their intrinsic properties as biomacromolecules that can be used to detect biological metabolites. Future efforts could focus on the development of aptamers for D-lactate and use such aptamers for practical biosensors that can be used for continuous monitoring. Third, simultaneous monitoring of lactate and LDH might be interesting since multiplexed detection can give more information on the physiological state of patients. Finally, incorporation of the affinity ligands with nanomaterials may further improve biosensor detection performance.[91–96]

## Conflicts of interest

There are no conflicts to declare.

## Data availability

No primary research results, software or code have been included and no new data were generated or analysed as part of this review.

## Acknowledgements

Funding for this work is from Natural Sciences and Engineering Research Council of Canada (NSERC) and the Canada Research Chairs (CRC) program.

## References

1 Q. Wang and T. Li, *Anal. Methods*, 2025, **17**, 7822–7845.
2 J. D. R. Schmidt, P. Walloch, B. Höger and E. Beitz, *Biochimie*, 2021, **188**, 7–11.
3 L. Messonnier, M. Kristensen, C. Juel and C. Denis, *J. Appl. Physiol.*, 2007, **102**, 1936–1944.
4 S. R. Bird, M. Linden and J. A. Hawley, *Ann. Clin. Biochem. Int. J. Lab. Med.*, 2014, **51**, 137–150.
5 I. A. Hashim, M. Mohamed, A. Cox, F. Fernandez and P. Kutscher, *Pract. Lab. Med.*, 2018, **12**, e00109.
6 S. M. Alshiakh, *SAGE Open Med.*, 2023, **11**, 20503121221136401.
7 R. Bou Chebl, C. El Khuri, A. Shami, E. Rajha, N. Faris, R. Bachir and G. Abou Dagher, *is Scand. J. Trauma Resusc. Emerg. Med.*, 2017, **25**, 69.
8 Y. M. Choi, H. Lim, H.-N. Lee, Y. M. Park, J.-S. Park and H.-J. Kim, *Biosensors*, 2020, **10**, 111.
9 P. J. Derbyshire, H. Barr, F. Davis and S. P. J. Higson, *J. Physiol. Sci.*, 2012, **62**, 429–440.
10 T.-T. Luo, Z.-H. Sun, C.-X. Li, J.-L. Feng, Z.-X. Xiao and W.-D. Li, *J. Physiol. Sci.*, 2021, **71**, 26.
11 E.-J. Jang, S.-M. Cha, S.-M. Choi and J.-D. Cha, *Arch. Oral Biol.*, 2014, **59**, 1233–1241.
12 A. C. Thomas, E. N. Potts, B. T. Chen, D. M. Slipetz, W. M. Foster and B. Driehuys, *NMR Biomed.*, 2009, **22**, 502–515.
13 S. Dokwal, A. Arya, A. Sachdeva, M. Rathi, S. Sachdeva, P. Prashant, V. Arora and J. Bhutani, *J. Clin. Diagn. Res.*, 2022, **16**, BC08–BC11.
14 S. Boterberg, E. Vantroys, B. De Paepe, R. Van Coster and H. Roeyers, *PLoS One*, 2022, **17**, e0274310.
15 A. B. Kharitonov, M. Zayats, L. Alfonta, E. Katz and I. Willner, *Sens. Actuators, B Chem.*, 2001, **76**, 203–210.
16 L. C. Clark, in *Methods in Enzymology*, Elsevier, 1979, vol. 56, pp. 448–479.
17 N. Nikolaus and B. Strehlitz, *Microchim. Acta*, 2008, **160**, 15–55.
18 V. G. Panferov, X. Zhang, K. Wong, J. H. Lee and J. Liu, *Angew. Chem., Int. Ed.*, 2025, **64**, e202512409.
19 W. Gao, X. Guan, J. Wang, N. F. Heinig, J. P. Thomas, L. Zhang, K. Ding and K. T. Leung, *ACS Appl. Nano Mater.*, 2024, **7**, 7162–7171.
20 M. Arivazhagan and G. Maduraiveeran, *Mater. Chem. Phys.*, 2023, **295**, 127084.
21 S. Kim, W. S. Yang, H.-J. Kim, H.-N. Lee, T. J. Park, S.-J. Seo and Y. M. Park, *Ceram. Int.*, 2019, **45**, 23370–23376.
22 S. Kim, K. Kim, H.-J. Kim, H.-N. Lee, T. J. Park and Y. M. Park, *Electrochim. Acta*, 2018, **276**, 240–246.
23 S. Jiang, X. Chen, J. Lin and P. Huang, *Adv. Mater.*, 2023, **35**, 2207951.
24 K. Rathee, V. Dhull, R. Dhull and S. Singh, *Biochem. Biophys. Rep.*, 2016, **5**, 35–54.
25 N. Rasitanon, S. Ittisoponpisan, K. Kaewpradub and I. Jeerapan, *Anal. Sens.*, 2023, **3**, e202200066.
26 D. S. Zia, Y. Chen and J. Liu, *Anal. Chem.*, 2026, **98**, 7515–7523.
27 P. J. Huang and J. Liu, *Angew. Chem., Int. Ed.*, 2023, **62**, e202212879.
28 L. Guo, Y. Song, Y. Yuan, J. Chen, H. Liang, F. Guo, Z. Yu, P. Liang, Y. Wang and P. Wang, *Anal. Bioanal. Chem.*, 2021, **413**, 4427–4439.
29 J. Kim, A. S. Campbell, B. E.-F. De Ávila and J. Wang, *Nat. Biotechnol.*, 2019, **37**, 389–406.
30 A. Fallah, A. A. Imani Fooladi, S. A. Havaei, M. Mahboobi and H. Sedighian, *Biochem. Biophys. Rep.*, 2024, **40**, 101852.
31 X. Chang, X. Chen, X. Zhang, N. Chen, W. Tang, Z. Zhang, S. Zheng, J. Huang, Y. Ji, Y. Zhao, Y. Yang and X. Li, *Biochem. Biophys. Res. Commun.*, 2024, **734**, 150449.
32 Y. Nasu, A. Aggarwal, G. N. T. Le, C. T. Vo, Y. Kambe, X. Wang, F. R. M. Beinlich, A. B. Lee, T. R. Ram, F. Wang, K. A. Gorzo, Y. Kamijo, M. Boisvert, S. Nishinami, G. Kawamura, T. Ozawa, H. Toda, G. R. Gordon, S. Ge, H. Hirase, M. Nedergaard, M.-E. Paquet, M. Drobizhev, K. Podgorski and R. E. Campbell, *Nat. Commun.*, 2023, **14**, 6598.
33 S. Tyagi and F. R. Kramer, *Nat. Biotechnol.*, 1996, **14**, 303–308.
34 B. Wang, J. Hong, C. Liu, L. Zhu and L. Jiang, *Sensors*, 2021, **21**, 8240.
35 Y. Inoue, A. Kuwahara, K. Ohmori, H. Sunayama, T. Ooya and T. Takeuchi, *Biosens. Bioelectron.*, 2013, **48**, 113–119.
36 G. Dykstra, I. Chapa and Y. Liu, *ACS Appl. Mater. Interfaces*, 2024, **16**, 66921–66931.
37 L. P. Sousa, L. A. M. Mariuba, R. J. Holanda, J. P. Pimentel, M. E. M. Almeida, Y. O. Chaves, D. Borges, E. Lima, J. L. Crainey, P. P. Orlandi, M. V. Lacerda and P. A. Nogueira, *BMC Infect. Dis.*, 2014, **14**, 49.
38 A. Schuck, M. Kang and Y.-S. Kim, *J. Electr. Eng. Technol.*, 2024, **19**, 3309–3316.
39 K.-Y. Wong, M.-S. Wong, J. H. Lee and J. Liu, *Adv. Drug Deliv. Rev.*, 2025, **224**, 115646.
40 H. Yu, O. Alkhamis, J. Canoura, Y. Liu and Y. Xiao, *Angew. Chem., Int. Ed.*, 2021, **60**, 16800–16823.
41 L. Wu, Y. Wang, X. Xu, Y. Liu, B. Lin, M. Zhang, J. Zhang, S. Wan, C. Yang and W. Tan, *Chem. Rev.*, 2021, **121**, 12035–12105.
42 S. Stangherlin, N. Lui, J. H. Lee and J. Liu, *TrAC, Trends Anal. Chem.*, 2025, **191**, 118349.
43 C. Tuerk and L. Gold, *Science*, 1990, **249**, 505–510.
44 A. D. Ellington and J. W. Szostak, *Nature*, 1990, **346**, 818–822.

45 M. Bozza, R. D. Sheardy, E. Dilone, S. Scypinski and M. Galazka, *Biochemistry*, 2006, **45**, 7639–7643.
46 M. Kohlberger and G. Gadermaier, *Biotechnol. Appl. Biochem.*, 2022, **69**, 1771–1792.
47 W. Zhou, R. Saran and J. Liu, *Chem. Rev.*, 2017, **117**, 8272–8325.
48 A. D. Ellington and J. W. Szostak, *Nature*, 1990, **346**, 818–822.
49 C. Tuerk and L. Gold, *Science*, 1990, **249**, 505–510.
50 M. Zuker, *Nucleic Acids Res.*, 2003, **31**, 3406–3415.
51 F. Bakhshandeh, H. Zheng, N. G. Barra, S. Sadeghzadeh, I. Ausri, P. Sen, F. Keyvani, F. Rahman, J. Quadrilatero, J. Liu, J. D. Schertzer, L. Soleymani and M. Poudineh, *Adv. Mater.*, 2024, **36**, 2313743.
52 Y. Liu, Y. Li, S. Zhang, D. Du, Y. Zhang, H. Shi, J. Ni, L. Xiang, H. Xu and Y. Zhang, *Biomaterials*, 2026, **331**, 124144.
53 M. D. Levitt and D. G. Levitt, *Clin. Exp. Gastroenterol.*, 2020, **13**, 321–337.
54 D. J. Herrera, K. Morris, C. Johnston and P. Griffiths, *Ann. Clin. Biochem. Int. J. Lab. Med.*, 2008, **45**, 177–183.
55 J. B. Ewaschuk, J. M. Naylor and G. A. Zello, *J. Nutr.*, 2005, **135**, 1619–1625.
56 Y. Nasu, C. Murphy-Royal, Y. Wen, J. N. Haidey, R. S. Molina, A. Aggarwal, S. Zhang, Y. Kamijo, M.-E. Paquet, K. Podgorski, M. Drobizhev, J. S. Bains, M. J. Lemieux, G. R. Gordon and R. E. Campbell, *Nat. Commun.*, 2021, **12**, 7058.
57 Y. Kamijo, P. Mächler, N. Ness, C. Q. Vu, T. Kusakizako, J. Mannuthodikayil, Z. Ku, M. Boisvert, E. Grebenik, I. Miyazaki, R. Hashizume, H. Sato, R. Liu, Y. Hori, T. Tomita, T. Katayama, A. Furube, G. Caraveo, M.-E. Paquet, M. Drobizhev, O. Nureki, S. Arai, M. Brancaccio, R. E. Campbell, D. Kleinfeld and Y. Nasu, *Nat. Commun.*, 2025, **16**, 9531.
58 X. Li, Y. Zhang, L. Xu, A. Wang, Y. Zou, T. Li, L. Huang, W. Chen, S. Liu, K. Jiang, X. Zhang, D. Wang, L. Zhang, Z. Zhang, Z. Zhang, X. Chen, W. Jia, A. Zhao, X. Yan, H. Zhou, L. Zhu, X. Ma, Z. Ju, W. Jia, C. Wang, J. Loscalzo, Y. Yang and Y. Zhao, *Cell Metab.*, 2023, **35**, 200–211e9.
59 J. Wojcieszek, I. Wojciechowska, J. Dominiczak, J. Krzemiński, A. Pepłowski and Ł. Górski, *Sens. Actuators, B Chem.*, 2024, **421**, 136475.
60 C. Alexander, H. S. Andersson, L. I. Andersson, R. J. Ansell, N. Kirsch, I. A. Nicholls, J. O'Mahony and M. J. Whitcombe, *J. Mol. Recognit.*, 2006, **19**, 106–180.
61 Y. Li, L. Luo, Y. Kong, Y. Li, Q. Wang, M. Wang, Y. Li, A. Davenport and B. Li, *Biosens. Bioelectron.*, 2024, **249**, 116018.
62 Y. Wang, C. Pang, X. Ma, M. Wang, X. Wu, S. Liu and S. Li, *Luminescence*, 2024, **39**, e4871.
63 X.-Y. He, Y. Wang, Q. Xue, W.-F. Qian, G.-L. Li and Q. Li, *Food Chem.: X*, 2025, **26**, 102322.
64 X. Xin, H. Liu, N. Zhong, M. Zhao, D. Zhong, H. Chang, B. Tang, Y. He, C. Peng and X. He, *Sens. Actuators, B Chem.*, 2022, **357**, 131468.
65 K. A. Birari, P. O. Patil, M. Taleuzzaman, M. S. Alam, S. Wahab, M. Khalid and Z. G. Khan, *Microchim. Acta*, 2025, **192**, 242.
66 S. Pei, W. Ji, Y. Yang, T. Liu, S. Yang, J. Wu, J. Dai, X. Hou, Q. Wu and L. Li, *Anal. Sens.*, 2024, **4**, e202400003.
67 E. Piskin, A. Cetinkaya, Z. Eryaman, L. Karadurmus, M. A. Unal, M. K. Sezgintürk, J. Hizal and S. A. Ozkan, *Microchem. J.*, 2024, **204**, 111163.
68 Y. L. Mustafa and H. S. Leese, *ACS Omega*, 2023, **8**, 8732–8742.
69 L. Zhou, *Int. J. Electrochem. Sci.*, 2021, **16**, 211043.
70 S. M. Mugo, S. V. Robertson and W. Lu, *Anal. Chim. Acta*, 2023, **1278**, 341714.
71 M. Wusiman and F. Taghipour, *Microsyst. Nanoeng.*, 2024, **10**, 175.
72 P. Kanokpaka, L.-Y. Chang, B.-C. Wang, T.-H. Huang, M.-J. Shih, W.-S. Hung, J.-Y. Lai, K.-C. Ho and M.-H. Yeh, *Nano Energy*, 2022, **100**, 107464.
73 Q. Zhang, D. Jiang, C. Xu, Y. Ge, X. Liu, Q. Wei, L. Huang, X. Ren, C. Wang and Y. Wang, *Sens. Actuators, B Chem.*, 2020, **320**, 128325.
74 X. Xuan, C. Pérez-Ràfols, C. Chen, M. Cuartero and G. A. Crespo, *ACS Sens.*, 2021, **6**, 2763–2771.
75 Y. Matos-Peralta and M. Antuch, *J. Electrochem. Soc.*, 2020, **167**, 037510.
76 Y. Chen, X. Hu, Q. Liang, X. Wang, H. Zhang, K. Jia, Y. Li, A. Zhang, P. Chen, M. Lin, L. Qiu, H. Peng and S. He, *Adv. Funct. Mater.*, 2024, **34**, 2401270.
77 K. Kogawa, S. Minakawa, Y. Matsuzaki, A. Okamoto, S. Ogasawara, N. Saito, D. Sawamura and J. Cutan, *Immunol. Allergy Clin. North Am.*, 2022, **5**, 133–135.
78 Y. Yuan, Y. Gu, X. Qu, Q. Shi, H. Bai, J. Xu, J. Xu, J. Li and L. Chen, *Blood*, 2016, **128**, 5637.
79 L. Lin, R. Gao, L. Chen, Z. Wu, X. Wei and Y. Xie, *Medicine*, 2022, **101**, e31499.
80 R. W. Oei, L. Ye, F. Kong, C. Du, R. Zhai, T. Xu, C. Shen, X. Wang, X. He, L. Kong, C. Hu and H. Ying, *J. Cancer*, 2018, **9**, 54–63.
81 L. Zhou, C. Li, Y. Luo, Q. Liang, Y. Chen, Z. Yan, L. Qiu and S. He, *Natl. Sci. Rev.*, 2025, **12**, nwaf155.
82 G. Xiao, J. He, Y. Qiao, F. Wang, Q. Xia, X. Wang, L. Yu, Z. Lu and C.-M. Li, *Adv. Fiber Mater.*, 2020, **2**, 265–278.
83 Y.-W. Cheung, J. Kwok, A. W. L. Law, R. M. Watt, M. Kotaka and J. A. Tanner, *Proc. Natl. Acad. Sci. U. S. A.*, 2013, **110**, 15967–15972.
84 S. Lee, D. H. Manjunatha, W. Jeon and C. Ban, *PLoS One*, 2014, **9**, e100847.
85 S. Lee, K.-M. Song, W. Jeon, H. Jo, Y.-B. Shim and C. Ban, *Biosens. Bioelectron.*, 2012, **35**, 291–296.
86 Y.-W. Cheung, R. M. Dirkzwager, W.-C. Wong, J. Cardoso, J. D'Arc Neves Costa and J. A. Tanner, *Biochimie*, 2018, **145**, 131–136.
87 Y.-J. Kim and J.-W. Choi, *RSC Adv.*, 2022, **12**, 29535–29542.
88 Q. Yang, J. Pedreira-Rincón, L. Balerdi-Sarasola, L. Baptista-Pires, J. Muñoz, D. Camprubí-Ferrer, A. Idili and C. Parolo, *Biosens. Bioelectron.*, 2025, **274**, 117152.
89 K.-A. Frith, R. Fogel, J. P. D. Goldring, R. G. E. Krause, M. Khati, H. Hoppe, M. E. Cromhout, M. Jiwaji and J. L. Limson, *Malar. J.*, 2018, **17**, 191.

90 Y. D. Banguera-Ordoñez, A. Sena-Torralba, P. Quintero-Campos, Á. Maquieira and S. Morais, *Talanta*, 2025, **281**, 126803.
91 W. Xu, W. He, Z. Du, L. Zhu, K. Huang, Y. Lu and Y. Luo, *Angew. Chem., Int. Ed.*, 2021, **60**, 6890–6918.
92 Y. Ding and J. Liu, *Chin. J. Chem.*, 2024, **42**, 2391–2400.
93 H. Song, D. H. Jung, Y. Cho, H. H. Cho, V. G. Panferov, J. Liu, J. H. Heo and J. H. Lee, *Coord. Chem. Rev.*, 2025, **541**, 216835.
94 L. Wu, Y. Wang, X. Xu, Y. Liu, B. Lin, M. Zhang, J. Zhang, S. Wan, C. Yang and W. Tan, *Chem. Rev.*, 2021, **121**, 12035–12105.
95 M. Zandieh, J. H. Lee and J. Liu, *Chem. Sci.*, 2025, **16**, 14865–14883.
96 J. Zhang, T. Lan and Y. Lu, *TrAC, Trends Anal. Chem.*, 2020, **124**, 115782.